Study of asphaltenes and sub-fraction nanoaggregates by AFM force spectroscopy

Vicmary Vargas, Jimmy Castillo, Brice Bouyssière, Carrier Hervé, Sadia Radji

Study of asphaltenes and sub-fraction nanoaggregates by AFM force spectroscopy

Vicmary Vargas [a,b], Jimmy Castillo[c], Brice Bouyssiere [a,b], Herve Carrier [b,d], Sadia Radji [a,b].*

[a] Universite de Pau et des Pays de l'Adour, E2S UPPA, CNRS, IPREM, Institut des Sciences Analytiques et de Physico-chimie pour l'Environnement et les Matériaux, UMR5254, Hélioparc, 64053 Pau, France.

[b]Joint Laboratory C2MC: Complex Matrices Molecular Characterization, Total Research & Technology, Gonfreville, BP 27, F-76700 Harfleur, France.

[c] Laboratorio de Espectroscopía Láser, Escuela de Química, Facultad de Ciencias, Universidad Central de Venezuela, Caracas, 1053, Venezuela.

[d] Universite de Pau et des Pays de l'Adour, E2S UPPA, CNRS, TOTAL, LFCR, UMR 5150, 64012 Pau, France.

1. INTRODUCTION.

Crude oil is a valuable, but extremely complex natural matrix resource. Asphaltenes are considered to be not only the most complex component but also the most troublesome. As the most aromatic and polar portion of crude oil, they have low solubility in low molecular weight paraffins such as pentane or n-heptane [1,2], but are soluble in benzene or toluene [3].

Furthermore asphaltenes, being the constituent of crude oil with the highest in molecular weights, possess a pronounced inclination to aggregate and form flocculates [4].

Understanding the structures at the nanometer scale can help understanding asphaltene deposition. The correlation between the configuration of asphaltene molecules and their influence on the adhesion and mechanical characteristics of deposits is not well understood [5]. The structure and molecular mass of asphaltene aggregates are not fully characterized at present. This is mainly due to the great heterogeneity of the molecules that compose them, as well as to the variations observed depending on the origin of the crude oil [3]. See for example the remarkable work by Schuler and al, from IBM and Princeton University, on isolated asphaltene molecules, at the molecular level, using scanning tunneling microscope (STM) coupled to atomic force microscope (AFM). However, this was under extreme conditions corresponding on an ultrahigh vaccum (~10^{-10} mba) at low temperature (~5 K). This study, focusing on the structure of the molecules composing asphaltene aggregates, showed that molecules of asphaltenes structures, depending on the origin of the crude, could be structured in the form of islands or archipelagos [6–9]. The island-type structure has a large nucleus and few branches, while the archipelago with aliphatic chains gives it greater flexibility and mobility.

"Island" type asphaltenes are the first proposed by Yen in 1961[10] and refined by Dickie and Yen in 1967, [11,12]. It consists of a single polyaromatic core that may or may not be stabilized by alkyl side chains. The second "archipelago" class, introduced by Strausz et al. in 1992 [13,14], features multiple aromatic cores cleaved by alkyl, aryl-aryl or cycloalkyl linkage[15]. Recent research has validated the coexistence of both the "island" and "archipelago" structures in asphaltenes, with the prevalence of one structure over the other being contingent upon the origin of the sample [15–17].

Two complementary mechanisms models currently are employed to describe the aggregation of asphaltenes. The Yen-Mullins colloidal model [18–20] and the supramolecular model proposed by Gray et al [21] are hierarchical suggesting that asphaltenes have a tendency to form compact nanoaggregates consisting of approximately ∼6 molecules. These nanoaggregates then further combine to create clusters composed of approximately ∼8 nanoaggregates [22]. González et al. specifically investigated the presence of asphaltene aggregates in Tetrahydrofuran (THF) solution and support the existence of small aggregates in the nanometer range[23]. The aggregation of asphaltenes is primarily driven by π-π stacking interactions between the aromatic cores, as well as van der Waals and dipole-dipole interactions.[24] These interactions are influenced by the presence of alkyl side chains, which contribute to steric repulsions and control the size of the nanoaggregates. However, according to Gray et al. [21] the Yen-Mullins model is unable to capture the complete complexity of the physical-chemical behavior exhibited by the asphaltene fraction. To address this, they proposed a supramolecular model that considers additional factors such as van der Waals interactions between alkyl groups, Coulomb-driven interactions, and hydrogen-bond networks. This supramolecular model provides a more comprehensive understanding of the aggregation process [4,21].

Earlier work [25–27] utilizing complex formation with p-nitrophenol (PNP), showed that asphaltenes can be separated into two subfractions with comparable molecular characteristics but contrasting solubilities in toluene. One subfraction, referred to as A1, is insoluble in toluene, while the other subfraction, A2, is soluble. These two subfractions exhibit distinct aggregation behaviors, highlighting the impact of solubility on their respective properties [28]. The fractionation process involves the formation of complexes with p-nitrophenol, which selectively solubilizes certain components and not others. The resulting insoluble fraction (A1) is considered a subfraction of

asphaltenes. Fraction A1 retains the characteristics associated with asphaltenes, such as high molecular weight and aggregation tendencies. Gutierrez et al.[29] describes the procedure in detail and showed that there is no chemical change in the components after separation. The method focuses on structural studies and stability analysis of asphaltene colloids. As discussed, Gutierrez et al, recovery yield close to 100% when done properly and following the proposed methodology. The analysis of each of the steps in the methodology shows that there is no chemical change in the fractions. A charge transfer complex is formed, which is then separated and the original molecules are recovered without chemical transformation. This leads to the separation of two fractions whose chemical composition is very similar but with important differences in macrocopic behavior such as solubility, which plays a very important role in the formation and stability of the aggregates.

On a molecular scale, multiple characterization techniques indicate that the A1 subfraction possesses a pronounced structural nature resembling islands. On the other hand, the A2 subfraction exhibits a character akin to archipelagos. These findings suggest that the two subfractions differ in terms of their molecular arrangements and the connectivity of aromatic cores within the asphaltene molecules [15]. According to Acevedo [28] the A1 subfraction, which is insoluble in toluene, plays a crucial role in initiating the nucleation of asphaltene aggregation through a Yen-Mullins mechanism. In their work they propose that the A2 subfraction, soluble in toluene, has the ability to stabilize small aggregates. Interestingly, when a few A2 molecules are introduced into nuclei primarily composed of A1 molecules, it hampers the growth of asphaltene aggregates and prevents phase separation. Therefore, A2 can be considered a stabilizing agent that induces a colloidal behavior in the system[4]. Recent work [30] presents a review of the experimental evidence supporting the existence of the so-called A1 and A2 fractions, as well as the spectroscopic data supporting their insular and archipelagic character.

Recent studies using molecular dynamic simulation show that asphaltenes with predominantly island characteristics (A1) form aggregates with strong π-π interactions which generate a dense and compact aggregate, while in archipelago-type asphaltenes (A2) van der Waals and hydrogen bonding's are important, due to the heteroatoms in their structure[4].

Atomic force microscopy (AFM) technique is a valuable tool for investigating surface phenomena. It offers a visual analysis of the structures formed by molecules under various conditions, providing information on their behavior at the nanoscale. AFM makes it possible to observe and characterize molecular structures, aggregates, and interactions with high resolution, contributing to a deeper understanding of surface-related phenomena [2,5,31]. AFM provides the ability to obtain three-dimensional images with extremely high spatial resolution, measuring in subnanometer scales [32]. AFM opers windows on both the structure [33] and the interactions of asphaltenes with various metallic [34–37] and mineral substrates [38,39], across diverse environmental circumstances, including aqueous, emulsion, and organic media, as well as different temperature settings [5]. In this work, we used an AFM to confirm the existence of nanoaggregates at very low dilutions in a good solvent as THF. Force spectroscopy mode was then used to probe the interaction of single asphaltenes and A1 and A2 subfraction nanoaggregates with the AFM tip. All three types of aggregate deposited on silica surface have different mechanical and structural properties. The results show an important difference in the structure of the asphaltene aggregates formed by A1 compared to those formed by A2, being the A1 aggregates are more compact than the A2 aggregates. These results, agree with those, obtained using molecular dynamics in recent studies[4]. This difference in their structures and interaction mechanisms is associated with the possibility of interaction with the solvent and thus with the formation and stability of the aggregates, and also

sheds light on the possible interaction mechanisms that allow changes in the stability of the aggregates in different solvents.

2. MATERIALS AND METHODS.

2.1. Reagents and Materials. The following solvents were used for the asphaltaene precipitation: toluene (99.8% purity, Scharlau), n-heptane (99% purity, Scharlau). For fractionation into the A1 and A2 subfractions: cumene (99%, Alfa Aesar), sodium hydroxide (synthesis grade, 98%, Scharlau) and p-nitrophenol (PNP, synthesis grade, 99%, Scharlau) were used. Finally, tetrahydrofuran (THF, ACS, stabilized with 250 mg L-1 of 2,6-di-tert-butyl 4-methylphenol (BHT), 99.9% purity, Scharlau) was used for the preparation of the solutions.

2.2. Asphaltene Separation. Whole asphaltenes in this study were acquired from three Venezuelan crude oils, specifically Hamaca, Cerro Negro, and Furrial, employing the method previously described [23,29,40,41] (based on the ASTM standard D6560-17). In summary, we induced precipitation by adding n-heptane to the crude oil in a volume ratio of 1:40. The mixture was then filtered, and a Soxhlet extraction was performed using n-heptane as the solvent for one week to eliminate any coprecipitated substances.

2.3. Asphaltene Fractionation. The asphaltenes fractionation here is based on the procedure reported by Acevedo [23,29,40,42].

Asphaltenes subfractions A1 and A2 were obtained by dissolving asphaltenes in a saturated solution of p-nitrophenol (PNP). The resulting mixture was refluxed for 6 hours and left to stand

at room temperature for a week. During this time, the A1 subfraction formed an insoluble asphaltene-PNP complex and precipitated out, while the A2 subfraction and trapped compounds (TC) remained in solution.

After filtration to separate the A1 subfraction, cumene was removed by distillation at reduced pressure. The resulting residue was washed with hot n-heptane to obtain the TC and A2 subfractions. Successive washings with 5% NaOH solutions were performed to remove PNP until colorless washings were obtained for both the A1 and A2 subfractions. This separation methodology involves successive washes and solvent evaporation, which can lead to small differences, especially in the trapped compounds, leading to errors of up to 10% in the total.

2.4. Preparation of asphaltene and fraction solution. Solutions of asphaltenes and their subfractions A1 and A2 from Hamaca, Cerro Negro and Furrial crude oils were prepared in THF at concentrations of 0,1 and 0,01mg L−1, and left to stand for 24 hours to ensure that the aggregates in solution are stable. Table 1 presents the previously reported asphaltene contents of the crude oils.[23,27]

Table 1. Crude oil samples and percentage of recovery in their fractionation.

CRUDE OIL	HAMACA	CERRO NEGRO	FURRIAL
API	9.0	8.5	24
% ASPHALTENES	13.7	8.0	4.0
% A1	38.0	20.0	48.0
%A2	58.0	72.0	46.0
% TRAPPED COMPOUNDS	3.0	6.0	3.0

2.5.AFM imaging and force spectroscopy modes. One A drop of each solution was evaporated on a previously cleaned silicon plate. THF was used as a good solvent and ensured that the evaporation process was rapid. To ensure, that the distance between the nanoaggregates, formed in the solution was sufficient, the solution was prepared at a very low concentration. Thus, the possibilities of aggregation during evaporation were minimized. This should make it possible to maintain the same structure of the aggregates in solution and on the substrate. The low surface tension of THF further discouraged the formation of aggregates. This method has been used successfully in previous work.[5,34]

Surface AFM images were acquired with a Multi-Mode VIII instrument (BRUKER) and Nanoscope 8.15 software. The Scan Assist Air mode was chosen for imaging the samples, with silicon nitride cantilevers with a calibrated spring constant of 0.72 ± 0.03 N/m and a typical tip radius of around 10 nm. Height was taken as a measure of size due to the challenge of correcting the X-Y dimensions for the size of the AFM tip (10 nm). All experiments were carried under air at room temperature. Force spectroscopy mode was performed on 5 nanoaggregates in each sample. All force spectroscopy measurements were performed at the same loading rate of 2,5μN/s.

3. RESULTS.

AFM imaging and Force spectroscopy revealed differences in the size distribution, and morphological and structural features of A1 and A2 asphaltene aggregates. We found that asphaltenes and their subfractions form 2-10 nm aggregates height, even at very high dilutions. The structure of these aggregates depends on their molecular organization, which depends of the crude oil's origin. Force spectroscopy was used to determine the mechanical response of the nanoaggregates, and to study the mechanical properties of the asphaltene subfraction segments.

For these experiments, aggregates with dimensions outside the common range (around 300 nm), were selected. This is to avoid the phenomena of sliding, of the AFM tip, on the surface of the aggregates.

3.1. AFM Images. Asphaltenes and their subfractions A1 and A2, were imaged in different region of the surface.

Figure 1 shows representative height images (1,5 µm × 1,5 µm) of the A1 and A2 Cerro Negro and Hamaca samples deposited on the silica substrate at low concentrations in THF. This solvent efficiently disperses asphaltenes and their A1 and A2 subfractions. Aggregates from all samples were of similar size, their heights ranging are mostly between 2 and 10 nm (Supplementary materials, Figure S1-S3). Some aggregates were larger up to 300 nm.

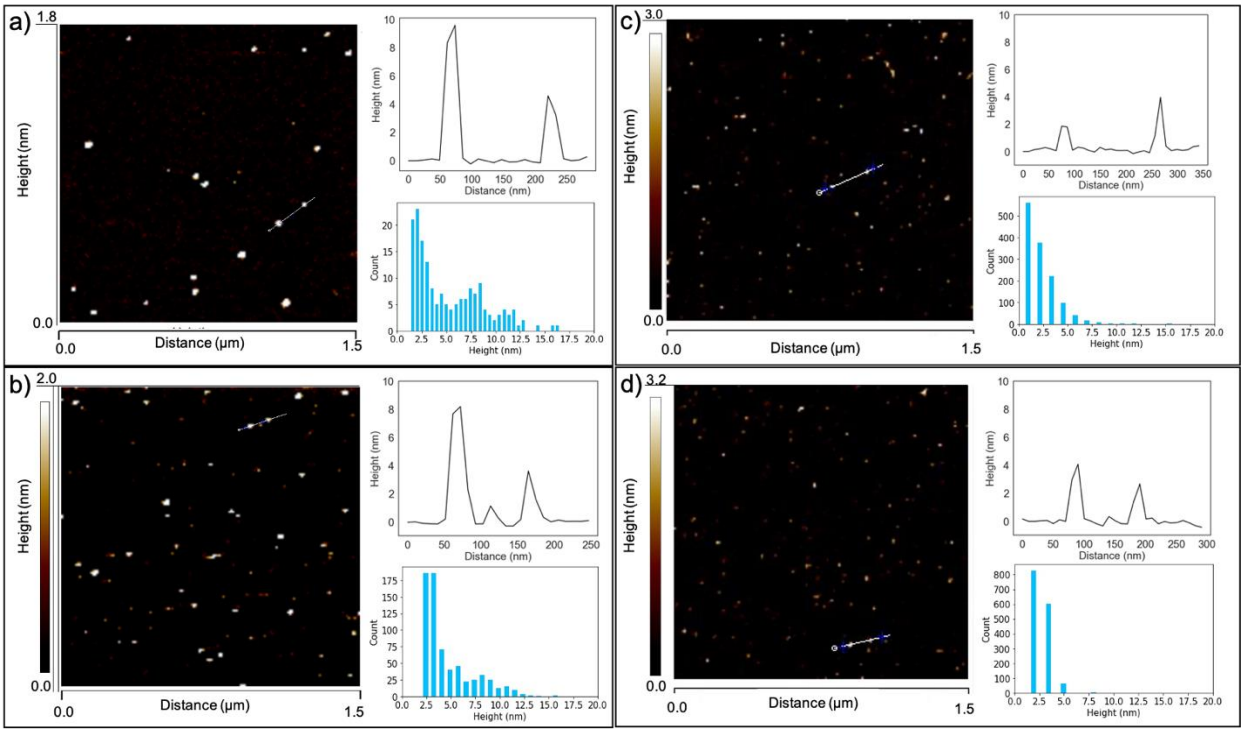

Figure 1. Representative AFM images height (1,5 μm × 1,5 μm), and cross-sections (white lines in the topography panels) and the height distributions of aggregates for a) A1 Cerro Negro sample and b) A2 Cerro Negro samples both deposited from 0,1ppm solution, c) A1 Hamaca and d) A2 Hamaca both deposited from 0,01ppm.

Distribution of size were similar at both concentrations used to deposit aggregates. The higher concentration used in all subsequent measurements was more convenient in providing a higher surface density of aggregates.

Figure 2 shows aggregate cross section extracted from the images. The intensity profile, in the plots, shown different characteristics, depending on the studied sample. For figure 2a a profile with flat zones is observed, these flat zones are associated with plane layers and consistent with the pi-pi interaction. In figure 2b the profile is continuum consistent with agglomeration of aggregates. The figure 2c present a mixture of both behaviors. Similar behavior was observed for the rest of the samples (Supplementary materials, Figure S4-S5).

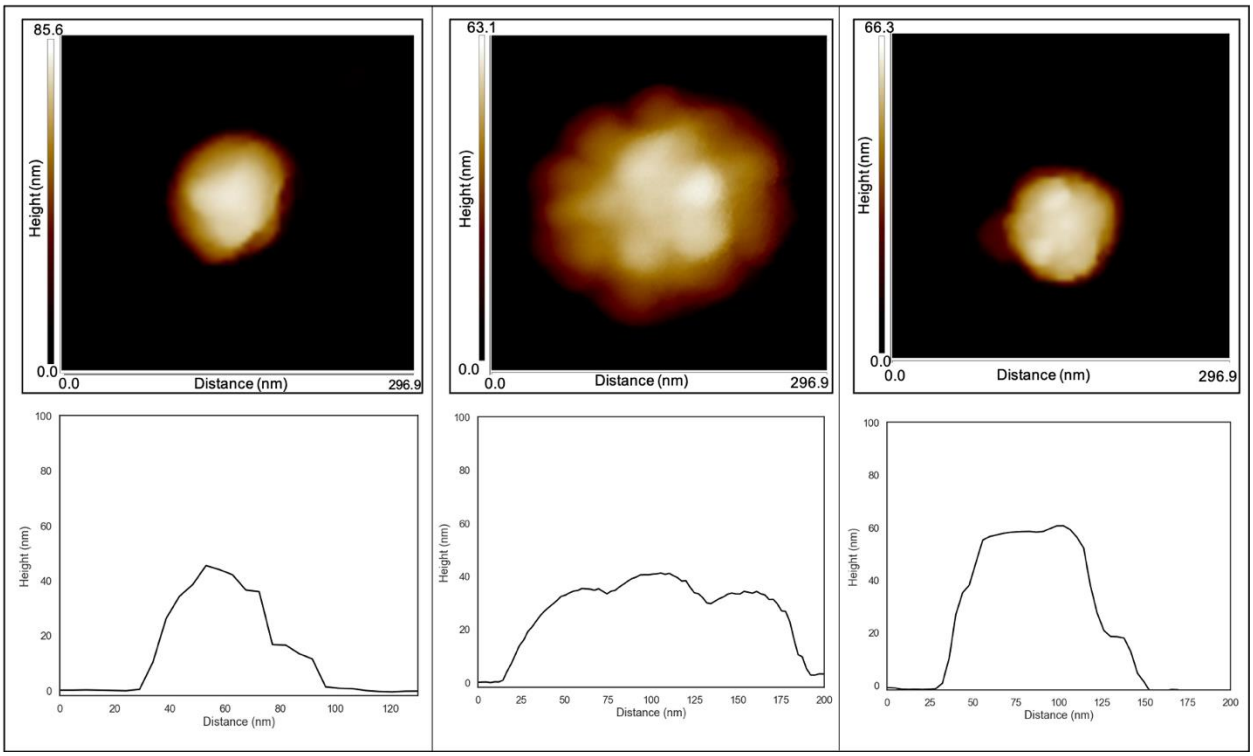

Figure 2. AFM images of different aggregation types a) in layers (A1 Hamaca sample), b) agglomeration of small spherical (A1 Furrial sample), c) mixture of layers and spheres (A1 Cerro Negro sample).

3.2. Mechanical properties of nanoaggregates. In this section, both mechanical characterization of various systems, and the determination of molecular of asphaltene subfraction segment elasticity, are discussed. In the AFM force spectroscopy experiments, a force curve was recorded, as function of the height of the tip, relative to the top of the aggregates. To avoid the tip for sliding, we selected broad nanoaggregates of 50-300 nm diameter, to force spectroscopy measurement.

Force spectroscopy is widely employed for evaluating local mechanical properties at the nanoscale [43]. In this mode, the piezoelectric scanner moves the cantilever base relative to the sample with a predefined vertical speed profile, the same during approach and retract phases. These

experiments are provided F-Z force curves, the relationship between the applied force and the displacement of the scanner. After processing, these force curves can be represented as force versus indentation (F-δ) curves, where the indentation depth is determined from the scanner displacement. Experiments were realized on all of the sample types. Two different behaviors were evidenced for A1 and A2 Furrial samples (Figure 3). Indeed, the force spectroscopy experiments conducted on the A1 Furrial samples demonstrated a distinct viscoelastic behavior, which was evident from the pronounced hysteresis observed between the approach and retract force curves (Figure 3). This hysteresis indicates that the sample exhibits time-dependent mechanical responses, characteristic of viscoelastic materials. On the contrary, for A2 Furrial samples, the approach and retract force curves were superimposed indicating the purely elastic response of samples (Figure 3b). In this case, no dissipative processes such as viscoelastic one is involved into the A2 samples. All other samples showed the classical mechanical profile (Figure S6), as obtained in Figure 3b. These two distinct behaviors indicate that the mechanical responses of A1 and A2 Furrial networks, composing the nanoaggregates compressed by the AFM tip during indentation, were significantly different.

Indeed, the stiffness of the network composing the structure of the aggregates, through the entanglement of asphaltene's segments, as indicated by the slope of the approach force curve in Figure 3, is higher for the A2 Furrial sample (40,37 N/m) than for the A1 Furrial sample (21,41 N/m). The dissipative characteristic observed in A1 Furrial samples likely originates from interactions between the segment within the network. Stress relaxation measurements could help unravel the molecular origin of this dissipation, but this topic falls beyond the scope of this study[44].

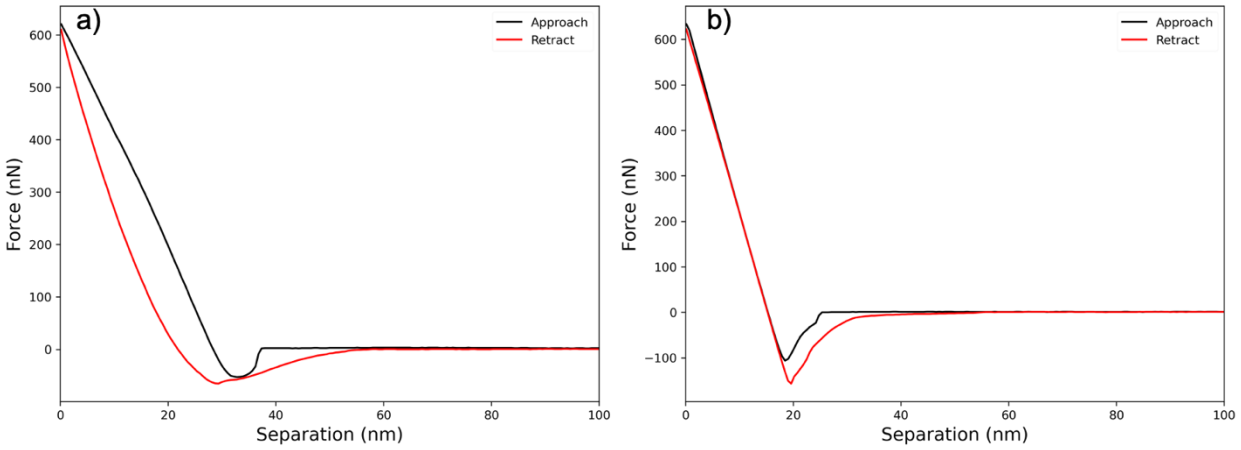

Figure 3. AFM force curves performed on a) A1 Furrial sample and b) A2 Furrial sample, realized with 2,5 µN/s loading rate.

In the second step, in order to compare the mechanical properties of individual segment of A1 and A2, using force spectroscopy mode, several cycles of approaching and retracting of the AFM tip on the bottom of nanoaggregates were realized. In the context of our study, the term "segment" here refers to an indefinite number of asphaltene molecules, e.g. at least 20 nm long in figure 4a. Some of these segments are present on the surface of the nanoaggregates, with one end free. Figure 4 shows the two types of profiles obtained from force spectroscopy experiments performed on the surface of nanoaggregates of asphaltene subfractions. The profile shown in Figure 4a corresponds to a force curve, performed on a surface with presence of free segment, and profile 4b corresponds to a force curve, performed on a surface without presence of free segment.

During the approach of the tip towards the surface of A1 and A2 nanoaggregates, the free end segments are in contact with the surface of the AFM tip. Then, the end of the segment physisorbs on the tip (Figure 4a). During the retract phase of force curve, the AFM cantilever moves away from the sample surface while having the end of the segment adsorbed on the tip. The segment is first unrolled, then stretched and finally desorbed from the AFM tip. Several (at least 50 for each

nanoaggregate) force curves have been recorded in the different sample. Only individual segments have been selected for the treatment to determine their molecular elasticity.

To begin, force peaks were observed during the retract phase from nanoaggregates, attributed to the detachment of a single segment attached to the AFM tip for A1 and A2 subfractions, as can be seen, on the peak surrounded by a blue circle, in Figure 4(a). The force measured through this peak, corresponding to the physisorption force of the segment on the AFM tip [45].

Then the same force curve profile, obtained in the same case of illustrated experiments in Figure 4(a), were fitted to obtain the elastic properties of individual segments. Precisely, the part corresponding of the unrolling and the stretching of individual segment, on the retract force curves, were fitted to an extended wormlike chain (WLC) model (Equation 1). The WLC model is commonly used to describe elastic properties of segments of organic assembly (DNA, Protein, polymer, etc), that exhibit behavior similar to that of wormlike polymer chains when subjected to an external load. In the context of asphaltene and asphaltene subfractions segments, their formation has been modeled using mechanisms that resemble linear polymerization. This involves linking small aromatic clusters together through aliphatic chains, analogous to the process of polymerization in linear polymers. The WLC model helps to explain the mechanical properties and behavior of asphaltene aggregates under external forces [5].

$$F(D) = \frac{k_B T}{l_p}\left[\frac{1}{4}\left(1 - \frac{D}{L} + \frac{F}{\phi}\right)^{-2} + \frac{D}{L} - \frac{F}{\phi} - \frac{1}{4}\right] \qquad \text{Equation (1)}$$

In equation 1, L is the contour length of the individual segments, related to the length of the segment, D is the tip displacement, lp is the persistence length and ϕ is the specific stiffness of the segment. Persistence length (lp) is measured in units of length. It represents the smallest non-deformable length that can constitute the segment. It quantifies the local stiffness of the segment. The parameter Φ corresponds to the overall stiffness of the segment. T is the absolute temperature,

corresponding to the room temperature (25°C) and k_B is the Boltzmann constant. The fit parameters are lp, ϕ and L.

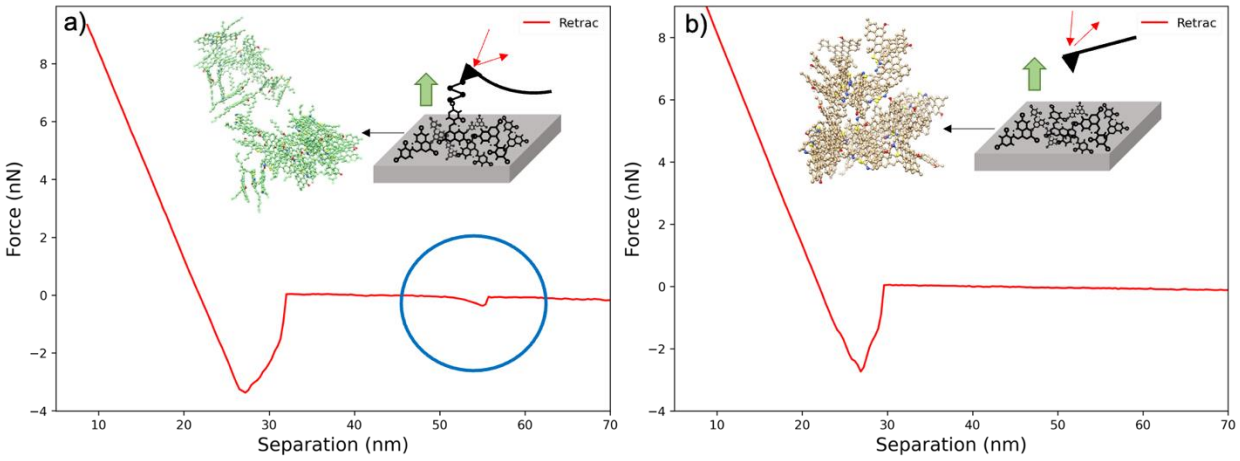

Figure 4. AFM retract force curves, obtained at the top of nanoaggregates a) A2 Cerro Negro profile with stretched segments and b) A1 Cerro Negro without stretched segments.

All retracted force curves realized on individual A1 and A2 subfraction segments could be fitted by the extended worm like chain model (WLC), giving an estimate of the contour length L. The elastic properties of a segment of the aggregate were well described by the WLC model [5,46], at least in a highly stretched region, and the adhesive force at the AFM tip was strong enough to extend the segments to approximately 94% of L. The distribution of L thus approximates the segment length distribution [47].

The parameter lp represents the local flexibility (or bending stiffness) of the segment. It is mainly determined by the lower part of the relatively flat part of the force curves. On the other hand, Ø primarily affects the upper portion of the curves, i.e., where force increases rapidly with extension until rupture. Therefore, lp and Ø are relatively independent of each other, and thus for each force curve, well defined values of lp and Ø are obtained[46]. By fitting the retract force curves with the

extended WLC model, as show in Figure 5, a specific stiffness (Ø) and a persistence length (lp) were obtained for A1 and for A2 segments.

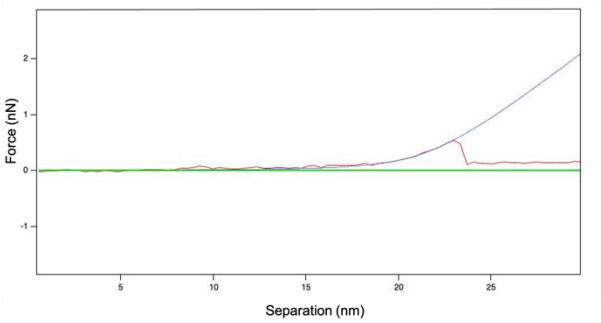

Figure 5. Retract A2 Cerro Negro force curve (red line), fitted with the extended WLC model (blue line).

Table 2 shows average results obtained by fitting the WLC model to retract force curves, which have the profile shown in Figure 4(a). Values of Ø and lp for A1 segments, are higher than for A2 segments, indicating that the former are stiffer. Acevedo and al[48]. propose that the structure of A1 is rigid and planar, whereas A2 is flexible and with branched aliphatic chain2s. They also suggest that A1 can form more stable hydrogen bonds. Combination of both interactions (π-π stacking and hydrogen bonds)[48], could explain the observed greater stiffness of A1 segments than that of A2. Pekerar and al[49], proposed two types of structures, to illustrate the difference in mobility of the supramolecular of asphaltenes, thus explaining their difference in rigidity. In this study, it was suggested that the rigidity is not due to a longer number of rings (aromatic groups), but rather to the way these rings are assembled together by aliphatic chains. In the case of a low mobility, the ring groups are larger and the number of aliphatic chains linking them would be lower, resulting in a more rigid structure. This rigid structure corresponds to the A1 segments. And in the case of easy mobility, clusters of small rings are attached together by longer aliphatic chains, resulting in a more flexible structure, with ease of rotation around C-C bonds. This flexible structure

corresponds to A2 segments. The structural models proposed by Acevedo and Pekerar [48,49], could explain the observed greater stiffness of A1 segments than that of A2.

Table 2. Mean and standard deviation of the adjustable parameters obtained in the fitting of the retract force curves with the extended WLC model.

SAMPLE	Specific stiffness, ø (N/m)	Persistence length, lp (nm)
A1	~9±0,02	~0,45±0,05
A2	~5,73±0,64	~0,21±0,04

4. DISCUSSION.

Except for the critical concentration, there is little information in the literature on asphaltene nanoaggregation. Fluorescence techniques revealed that even at low concentration, asphaltene molecules in toluene tend to form associations[50]. Extensive information on asphaltene nanostructures has been provided by techniques like small-angle X-ray scattering (SAXS) and small-angle neutron scattering (SANS) [20]. Consistent with the Yen-Mullins model[19,20], Figure 1 shows the presence of nanoaggregates and clusters at very low concentrations for both A1 and A2 solutions, as well as for asphaltene at high dilution in THF, where a size distribution from approximately 2 to 10 nm was shown previously [23] .The relative stability of the aggregates in solvents such as toluene, chloroform, and the original petroleum mixture has been exhibited. Heterogeneity has been evaluated by various analytical methods, revealing an average aggregate size ranging from 2 to 20 [6], as found here by AFM. Evidence suggests a polydisperse distribution [51]. Additional theories suggest the presence of supramolecular assemblies. Our data support, this hypothesis. Gray et al.[21] proposed distinct driving forces for supramolecular assembly involving

polar and aromatic group interactions. It is widely acknowledged that asphaltenes form aggregates, even in highly diluted solutions of compatible solvents like toluene or THF, as demonstrated in this study at concentrations of 0,1 mg/L in THF. Based on the available literature, it has been observed that asphaltenes appear in solution as aggregated structures at concentrations lower than 100 mg/L [50] which corresponds to our experimental observations. The small size of these nanoaggregates is believed to be due to steric hindrance caused by the alkyl chains surrounding the aromatic cores. From a colloidal standpoint, the critical nanoaggregate concentration represents the concentration at which the formation of nanoaggregates initiates. At higher concentrations (2-10 g/L), these nanoaggregates further associate to form clusters or micelles. These aggregates and clusters are commonly referred to as nano-colloidal and colloidal structures [27], respectively, and it is for this reason that we have chosen to work at really low concentration.

Different aggregation types were reported in the literature, aggregation in layers, by agglomeration of small spherical nanoaggregates and finally a mixture of layers and spheres. As shown in Figure 2a, aggregation is well-organized in layers, suggesting that the main interaction molecules might be π- π stacking between the aromatic cores. Conversely, spherical aggregates (Figure 2b), exhibit a lower level of spatial organization, suggesting that their aggregation is less influenced by π-π interactions. Instead, it aligns more closely with the supramolecular network structures proposed by Gray et al. [21]. These results are consistent with those reported in previous work[52], where predominant structures or their mixtures were observed. Depending on the separation process used and the origin of the samples, the structure of the aggregate depends if the process is controlled by diffusion of the small aggregates in the solution or instead for interaction of actives groups in the surface of the aggregates [46].

Rheological studies of, asphaltene and separated asphaltene fractions are rare. The studies carried out, have shown, that the rheological properties of asphaltenes, are influenced by the concentration, composition, precipitation/agglomeration and emulsification, the level of oxidation, as well as by time and pH [53-56]. These studies are still being researched in the literature at present. Here viscoelastic behavior (hysteresis of force curves), was observed only for the A1 Furrial samples. This observation allows us to infer that the viscoelasticity of asphaltenes depends on the origin of the oil and more particularly on the rate of presence of one of the sub-fractions.

The measurable properties of asphaltenes and their subfractions A1 and A2 from different sources, including elemental composition, functional group content, and density, have been observed to be similar. However, their molecular structure may vary. Figure 6 shows a hypothetical structure for asphaltenes A1 and A2 and asphaltene aggregates by mixing the hypothetical structures of A1 and A2 at 50%.[57,58] These molecular models were used by Villegas et all to study the interparticle interaction using the molecular dynamics calculations to model the aggregation of asphaltene and their subfractions. The paper describes in detail the interactions between the molecules to form aggregates and the importance of hydrogen bonding in the aggregate formation. Figure 6 shown the employed models showing the heteroatoms responsible of the charge interaction and the aromatic core responsible of pi-pi interaction. The figure illustrates that asphaltene aggregates are formed by different intermolecular forces, which include van der Waals forces as well as hydrogen bonds, as discussed in the previous works [57,58]. The aggregate illustrated in the Figure 6, shown a low-density structure, with polar groups in the surface, this characteristic allows the interaction of the aggregate with the AFM tip and the availability to deform the aggregate structure.

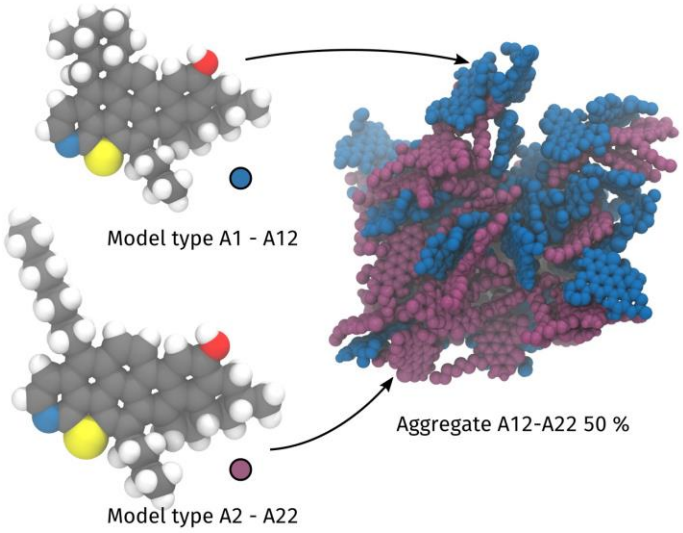

Figure 6. Molecular models of A1 and A2, and molecular dynamics simulation results, by mixing the hypothetical structures of A1 and A2 at 50% in THF [57].

All the mechanical properties are directly related to the aggregate structure, which depends on the aggregation mechanisms. Therefore, the present results provide information on the structure of the aggregates of subfractions A1 and A2. The data presented are in the order of magnitude reported in previous work [46], and are consistent with literature on the structure of A1 and A2 fractions, indicating that A2 is more flexible than A1 [4,23,28,49]. According to the findings of Acevedo et al.[28] , NMR analysis did not reveal significant distinctions between asphaltenes and their A1 and A2 subfractions. This study show that the resemblances observed in the Molecular Modeling distributions and the 13C NMR analysis, along with minor differences detected in the elemental analysis, indicate the presence of structural variations. The molecular models propose the opening of two aliphatic rings in A1 to form A2, highlighting that the 13C NMR technique is unable to differentiate between aliphatic (open chains) and alicyclic (ring chains) carbons. The sample data and the proposed mean structure are consistent with the experimental data obtained [28].

If A1 aggregates are formed by stacking flat structures as asserted Acevedo et al [28], they could be more difficult to stretch when picked up by the AFM tip, compared to A2. Aggregates of this type (A1) behave like a rigid object during stretching force from the AFM lever, which was conducted during the retract phase of force curve. Stretch-force curves obtained for the undefined A1 and A2 subfraction segments, were well fitted by the WLC model, in the same way as reported in other studies [5,46]. The values of the persistence length, representing the flexural stiffness and the stiffness Ø of A2 subfraction segment, are lower than that of A1, as is shown in table 2. These results are consistent with what is shown in the literature[48], showing that the A1 segments are more rigid than those of A2, which presents greater flexibility.

5. CONCLUSION.

In the present study, the AFM technique was used to observe and confirm the different types of aggregates in asphaltene samples of different origins, as well as their A1 and A2 subfractions, finding important differences that can be related to the different aggregation mechanisms. Using force spectroscopy in AFM, viscoelastic behavior was observed in some samples depending on the origin of the crude oil. Stress relaxation measurements could help unravel the molecular origin of this behavior, but this topic falls beyond the scope of this study[44].

Force curves representing the stretching of individual segments of A1 and A2 subfractions were obtained and were well fitted by the Worm Like Chain model, indicating that some of these aggregates acted as long-chain polymers under the pull of an external force. A2 segments showed lower flexural stiffness than A1 segments. This difference could be explained by the structural differences, proposed by Pekerar and al.[49] In the case of low mobility (A1), the cyclic groups are larger and the number of aliphatic chains connecting them would be lower, which would result in

a more rigid structure. And in the case of easy mobility (A2), groups of small rings are linked together by longer aliphatic chains, resulting in a more flexible structure, with easy rotation around the C-C bonds. Acevedo et al[48] also suggests that A1 is rigid and planar, with a predominance of π-π type bonds, with more stable hydrogen bonds than in A2. The combination of the two interactions (π-π stacking and hydrogen bonds) could also explain the greater rigidity of A1 compared to that of A2.

As part of this study, we chose to use a silicon substrate for the deposition of the aggregates, because silicon has a surface of low polarity and orientation. In order to continue to elucidate the mechanism of formation of asphaltene aggregates, and in order to understand how the nature of the substrate can orient the shape, size and structure, as well as the mechanical properties of the aggregates, we are currently continuing this study, in using substrates with different surface properties.

ESSENTIAL TITLE PAGE INFORMATION

Title

Study of asphaltenes and sub-fraction nanoaggregates by AFM force spectroscopy.

Author names and affiliations.

Vicmary Vargas [a,b], *Jimmy Castillo* [c], *Brice Bouyssiere* [a,b], *Herve Carrier* [b,d], *Sadia Radji* [a,b *].

[a] Universite de Pau et des Pays de l'Adour, E2S UPPA, CNRS, IPREM, Institut des Sciences Analytiques et de Physico-chimie pour l'Environnement et les Matériaux, UMR5254, Hélioparc, 64053 Pau, France.

[b]Joint Laboratory C2MC: Complex Matrices Molecular Characterization, Total Research & Technology, Gonfreville, BP 27, F-76700 Harfleur, France.

[c] Laboratorio de Espectroscopía Láser, Escuela de Química, Facultad de Ciencias, Universidad Central de Venezuela, Caracas, 1053, Venezuela.

[d] Universite de Pau et des Pays de l'Adour, E2S UPPA, CNRS, TOTAL, LFCR, UMR 5150, 64012 Pau, France.

Corresponding Author

Sadia Radji. Universite de Pau et des Pays de l'Adour, E2S UPPA, CNRS, IPREM, Institut des Sciences Analytiques et de Physico-chimie pour l'Environnement et les Matériaux, UMR5254, Hélioparc, 64053 Pau, France

E-mail : sadia.radji@univ-pau.fr

ABSTRACT

Asphaltenes, which are the most polar components found in crude oil, pose numerous challenges to the oil industry, during production, transport, and refining operations. In order to better understand their behavior and properties, specially the tendency to form aggregates, different methods have been tested to separate asphaltenes into subfractions. Among them, treatment with p-nitrophenol produces two subclasses: the A1 and A2 subfractions. These subclasses are similar in elemental composition but differ in solubility, structure and physicochemical behavior. In this work we study the difference in structuring between A1 and A2 at nanometer scale, confirming that in all cases the aggregates formed at very low concentrations (0.1 mg/L) have dimensions mostly between 2 and 10 nm. We measured the interaction between the atomic force microscope (AFM) tip and the aggregates, using force spectroscopy mode. In this study, the mechanical properties of the A1 and A2 nanoaggregates have been determined, as well as the mechanical properties of asphaltene subfraction segment.

GRAPHICAL ABSTRACT

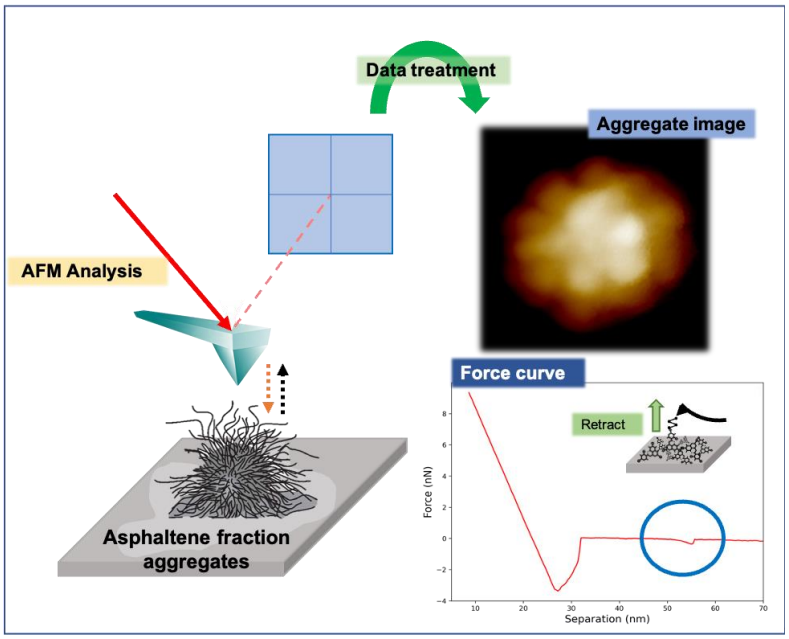

KEYWORDS. Atomic Force microscopy, asphaltenes, crude oil.

ABBREVIATIONS

AFM, Atomic force microscopy; PNP, p-nitrophenol; THF, tetrahydrofuran; TC, trapped compounds; WLC, wormlike chain.

ACKNOWLEDGMENT

The financial support provided by the ISIFOR Project A1A2-AFM is gratefully acknowledged.

FORMATTING OF FUNDING SOURCES

Funding: “Institut CARNOT” supported this work with ISIFOR project (A1A2-AFM).

REFERENCES

(1) Castillo, J.; Vargas, V.; Gonzalez, G.; Ruiz, W.; Gascon, G.; Bouyssiere, B. Development of a Methodology Using GPC-ICP HR MS for Analysis of the Adsorption of Asphaltene Aggregates on SiO2Nanoparticles. *Energy and Fuels* **2020**, 34 (6), 6920–6927.

(2) Oliveira, I.; Gomes, L.; Franceschi, E.; Borges, G.; de Conto, J. F.; Albuquerque, F. C.; Dariva, C. Surface and Interface Characterization of Asphaltenic Fractions Obtained with Different Alkanes: A Study by Atomic Force Microscopy and Pendant Drop Tensiometry. *Energy and Fuels* **2018**, 32 (12), 12174–12186.

(3) Acevedo, N.; Vargas, V.; Piscitelli, V.; le Beulze, A.; Bouyssiere, B.; Carrier, H.; Castillo, J. SiO2Biogenic Nanoparticles and Asphaltenes: Interactions and Their Consequences Investigated by QCR and GPC-ICP-HR-MS. *Energy and Fuels* **2021**, 35 (8), 6566–6575.

(4) Villegas, O.; Salvato Vallverdu, G.; Bouyssiere, B.; Acevedo, S.; Castillo, J.; Baraille, I. Molecular Cartography of A1 and A2 Asphaltene Subfractions from Classical Molecular Dynamics Simulations. *Energy and Fuels* **2020**, 34 (11), 13954–13965.

(5) Raj, G.; Lesimple, A.; Whelan, J.; Naumov, P. Direct Observation of Asphaltene Nanoparticles on Model Mineral Substrates. *Langmuir* **2017**, 33 (25), 6248–6257.

(6) Schuler, B.; Meyer, G.; Peña, D.; Mullins, O. C.; Gross, L. Unraveling the Molecular Structures of Asphaltenes by Atomic Force Microscopy. *J Am Chem Soc* **2015**, 137 (31), 9870–9876.

(7) Schuler, B.; Zhang, Y.; Collazos, S.; Fatayer, S.; Meyer, G.; Pérez, D.; Guitián, E.; Harper, M. R.; Kushnerick, J. D.; Peña, D.; Gross, L. Characterizing Aliphatic Moieties in Hydrocarbons with Atomic Force Microscopy. *Chem Sci* **2017**, 8 (3), 2315–2320.

(8) Schuler, B.; Fatayer, S.; Meyer, G.; Rogel, E.; Moir, M.; Zhang, Y.; Harper, M. R.; Pomerantz, A. E.; Bake, K. D.; Witt, M.; Peña, D.; Kushnerick, J. D.; Mullins, O. C.; Ovalles, C.; Van Den Berg, F. G. A.; Gross, L.; Kushnerick, T.; J Douglas, J. Heavy Oil Based Mixtures of Different Origins and Treatments Studied by AFM. *Energy and Fuels* **2017**, 31 (7), 6856–6861.

(9) Chen, P.; Metz, J. N.; Mennito, A. S.; Merchant, S.; Smith, S. E.; Siskin, M.; Rucker, S. P.; Dankworth, D. C.; Kushnerick, J. D.; Yao, N.; Zhang, Y. Petroleum Pitch: Exploring a 50-Year Structure Puzzle with Real-Space Molecular Imaging. *Carbon NY* **2020**, 161, 456–465.

(10) Yen, T. F.; Erdman, G.; Pollack Sidney. Investigation of the Structure of Petroleum Asphaltenes by X-Ray Diffraction. *Analytical Chemistry*, **1961**, Vol. 33(11), 1587-1594.

(11) Dickie, J. P.; Fu Yen, T. Macrostructures of the Asphaltic Fractions by Various Instrumental Methods. *Analytical Chemistry*, **1967**, Vol. 39(14), 1847-1852.

(12) Moir, M. E. Asphaltenes, What Art Thou? Asphaltenes and the Boduszynski Continuum: Contributions to the Understanding of the Molecular Composition of Petroleum. *American Chemical Society*, **2018**. Chapter 1, 3-24.

(13) Mojelsky, T. W.; Ignasiak, T. M.; Frakman, Z.; McIntyre, D. D.; Lown, E. M.; Montgomery, D. S.; Strausz, P. Structural Features of Alberta Oil Sand Bitumen and Heavy Oil Asphaltenes. *Energy Fuels* **1992, 6(1),** 83-96.

(14) Strausz, O. P.; Mojelsky, T. W.; Lown, E. M. The Molecular Structure of Asphaltene: An Unfolding Story. *Fuel* **1992**, 71(12), 1355-1363.

(15) Chacón-Patiño, M. L.; Rowland, S. M.; Rodgers, R. P. Advances in Asphaltene Petroleomics. Part 1: Asphaltenes Are Composed of Abundant Island and Archipelago Structural Motifs. *Energy and Fuels* **2017**, 31 (12), 13509–13518.

(16) Chacón-Patiño, M. L.; Rowland, S. M.; Rodgers, R. P. Advances in Asphaltene Petroleomics. Part 2: Selective Separation That Reveals Fractions Enriched in Island and Archipelago Motifs by Mass Spectrometry. *Energy and Fuels* **2017**, 31 (12), 13509–13518.

(17) Chacón-PatinÌo, M. L.; Rowland, S. M.; Rodgers, R. P. Advances in Asphaltene Petroleomics. Part 3. Dominance of Island or Archipelago Structural Motif Is Sample Dependent. *Energy and Fuels* **2018**, 32 (9), 9106–9120.

(18) Mullins, O. C.; Betancourt, S. S.; Cribbs, M. E.; Dubost, F. X.; Creek, J. L.; Andrews, A. B.; Venkataramanan, L. The Colloidal Structure of Crude Oil and the Structure of Oil Reservoirs. *Energy and Fuels* **2007**, 21 (5), 2785–2794.

(19) Mullins, O. C. The Modified Yen Model. *Energy and Fuels* **2010**, 24(4), 2179–2207.

(20) Mullins, O. C.; Sabbah, H.; Eyssautier, J.; Pomerantz, A. E.; Barré, L.; Andrews, A. B.; Ruiz-Morales, Y.; Mostowfi, F.; McFarlane, R.; Goual, L.; Lepkowicz, R.; Cooper, T.; Orbulescu, J.; Leblanc, R. M.; Edwards, J.; Zare, R. N. Advances in Asphaltene Science and the Yen-Mullins Model. *Energy and Fuels* **2012**, 26(7), 3986–4003.

(21) Gray, M. R.; Tykwinski, R. R.; Stryker, J. M.; Tan, X. Supramolecular Assembly Model for Aggregation of Petroleum Asphaltenes. *Energy and Fuels* **2011**, 25 (7), 3125–3134.

(22) Headen, T. F.; Boek, E. S.; Skipper, N. T. Evidence for Asphaltene Nanoaggregation in Toluene and Heptane from Molecular Dynamics Simulations. *Energy and Fuels* **2009**, 23(13), 1220–1229.

(23) González, G.; Acevedo, S.; Castillo, J.; Villegas, O.; Ranaudo, M. A.; Guzmán, K.; Orea, M.; Bouyssiere, B. Study of Very High Molecular Weight Cluster Presence in THF Solution of Asphaltenes and Subfractions A1 and A2, by Gel Permeation Chromatography with Inductively Coupled Plasma Mass Spectrometry. *Energy and Fuels* **2020**, 34 (10), 12535–12544.

(24) Pacheco-Sánchez, J. H.; Álvarez-Ramírez, F.; Martínez-Magadán, J. M. Morphology of Aggregated Asphaltene Structural Models. *Energy and Fuels* **2004**, 18 (6), 1676–1686.

(25) Acevedo, S.; Castro, A.; Vásquez, E.; Marcano, F.; Ranaudo, M. A. Investigation of Physical Chemistry Properties of Asphaltenes Using Solubility Parameters of Asphaltenes and Their Fractions A1 and A2. *Energy and Fuels* **2010**, 24 (11), 5921–5933.

(26) Mozes, E.; Delgado-Linares, J. G.; Cárdenas, A. L.; Salazar, F.; Pereira, J. C.; Bullón, J. Behavior of Asphaltene and Asphaltene Fractions Films on a Langmuir–Blodgett Trough and Its Relationship with Proposed Molecular Structures. *Pet Sci Technol* **2018**, 36 (18), 1490–1496.

(27) Castillo, J.; Gonzalez, G.; Bouyssiere, B.; Vargas, V. Asphaltenes, Subfractions A1 and A2 Aggregation and Adsorption onto RH-SiO2 Nanoparticles: Solvent Effect on the Aggregate Size. *Fuel* **2023**, 331(1), 125635.

(28) Acevedo, S.; Castillo, J.; Vargas, V.; Castro, A.; Delgado, O.; Cortés, F. B.; Franco, C. A.; Bouyssiere, B. Suppression of Phase Separation as a Hypothesis to Account for Nuclei or Nanoaggregate Formation by Asphaltenes in Toluene. *Energy and Fuels* **2018**, 32 (6), 6669–6677.

(29) Gutiérrez, L. B.; Ranaudo, M. A.; Méndez, B.; Acevedo, S. Fractionation of Asphaltene by Complex Formation with P-Nitrophenol. A Method for Structural Studies and Stability of Asphaltene Colloids. *Energy and Fuels* **2001**, 15 (3), 624–628.

(30) Acevedo, S.; Castillo, J. Asphaltenes: Aggregates in Terms of A1 and A2 or Island and Archipielago Structures. *ACS Omega* **2023**, (8)5, 4453–447.

(31) Beraldo, L.; Balestrin, S.; Cardoso, B.; Loh, W. Using Atomic Force Microscopy to Detect Asphaltene Colloidal Particles in Crude Oils. *Energy & Fuels* **2017**, Vol. 31 (4), 3738-3746.

(32) Garcia, R.; Perez, Ruben. Dynamic Atomic Force Microscopy Methods. *Surface Science Reports* **2002**, 47(6-8), 197-301.

(33) Wang, Y.; Zhao, K. Analysis of Nanoscale Microstructures in Asphalts of Different Aging States. *Journal of Materials in Civil Engineering* **2016**, 28 (1).

(34) Castillo, J.; Vargas, V.; Piscitelli, V.; Ordoñez, L.; Rojas, H. Study of Asphaltene Adsorption onto Raw Surfaces and Iron Nanoparticles by AFM Force Spectroscopy. *J Pet Sci Eng* **2017**, 151, 248–253.

(35) Ortega-Rodriguez, A.; Cruz, S. A.; Garcia-Cruz, I.; Lira-Galeana, C. Study of the Adhesion Force of Asphaltene Aggregates to Metallic Surfaces of Fe and Al. *Energy and Fuels* **2016**, 30 (5), 3596–3604.

(36) Zahabi, A.; Gray, M. R.; Dabros, T. Heterogeneity of Asphaltene Deposits on Gold Surfaces in Organic Phase Using Atomic Force Microscopy. *Energy and Fuels* **2012**, 26 (5), 2891–2898.

(37) Balabin, R. M.; Syunyaev, R. Z.; Schmid, T.; Stadler, J.; Lomakina, E. I.; Zenobi, R. Asphaltene Adsorption onto an Iron Surface: Combined near-Infrared (NIR), Raman, and AFM Study of the Kinetics, Thermodynamics, and Layer Structure. *Energy and Fuels* **2011**, 25 (1), 189–196.

(38) Acevedo, S.; Castillo, J.; del Carpio, E. H. Precipitation of Asphaltenes and Resins at the Toluene-Silica Interface: An Example of Precipitation Promoted by Local Electrical Fields Present at the Silica-Toluene Interface. *Energy and Fuels* **2014**, 28 (8), 4905–4910.

(39) Gonzalez, V.; Taylor, S. E. Asphaltene Adsorption on Quartz Sand in the Presence of Pre-Adsorbed Water. *J Colloid Interface Sci* **2016**, 480, 137–145.

(40) Acevedo, S.; Guzmán, K.; Labrador, H.; Carrier, H.; Bouyssiere, B.; Lobinski, R. Trapping of Metallic Porphyrins by Asphaltene Aggregates: A Size Exclusion Microchromatography with High-Resolution Inductively Coupled Plasma Mass Spectrometric Detection Study. *Energy and Fuels* **2012**; Vol. 26, 4968–4977.

(41) Orea, M.; Ranaudo, M. A.; Lugo, P.; López, L. Retention of Alkane Compounds on Asphaltenes. Insights about the Nature of Asphaltene-Alkane Interactions. *Energy and Fuels* **2016**, 30 (10), 8098–8113.

(42) Acevedo, S.; Cordero T., J. M.; Carrier, H.; Bouyssiere, B.; Lobinski, R. Trapping of Paraffin and Other Compounds by Asphaltenes Detected by Laser Desorption Ionization-Time of Flight Mass Spectrometry (LDI-TOF MS): Role of A1 and A2 Asphaltene Fractions in This Trapping. *Energy and Fuels* **2009**, 23 (2), 842–848.

(43) Efremov, Y. M.; Wang, W. H.; Hardy, S. D.; Geahlen, R. L.; Raman, A. Measuring Nanoscale Viscoelastic Parameters of Cells Directly from AFM Force-Displacement Curves. *Sci Rep* **2017**, 7 (1), 1–14.

(44) Cuenot, S.; Gélébart, P.; Sinquin, C.; Colliec-Jouault, S.; Zykwinska, A. Mechanical Relaxations of Hydrogels Governed by Their Physical or Chemical Crosslinks. *J Mech Behav Biomed Mater* **2022**, 133.

(45) Radji, S.; Alem, H.; Demoustier-Champagne, S.; Jonas, A. M.; Cuenot, S. Investigation of Thermoresponsive Nano-Confined Polymer Brushes by AFM-Based Force Spectroscopy. *Macromol Chem Phys* **2012**, 213 (5), 580–586.

(46) Long, J.; Xu, Z.; Masliyah, J. H. Single Molecule Force Spectroscopy of Asphaltene Aggregates. *Langmuir* **2007**, 23 (11), 6182–6190.

(47) Yamamoto, S.; Tsujii, Y.; Fukuda, T. Atomic Force Microscopic Study of Stretching a Single Polymer Chain in a Polymer Brush. *Macromolecules* **2000**, 33 (16), 5995–5998.

(48) Acevedo, S.; Escobar, O.; Echevarria, L.; Gutiérrez, L. B.; Méndez, B. Structural Analysis of Soluble and Insoluble Fractions of Asphaltenes Isolated Using the PNP Method. Relation between Asphaltene Structure and Solubility. *Energy and Fuels* **2004**, 18 (2), 305–311.

(49) Pekerar, S.; Lehmann, T.; Méndez, B.; Acevedo, S. Mobility of Asphaltene Samples Studied by 13C NMR Spectroscopy. *Energy and Fuels* **1999**, 13 (2), 305–308.

(50) Goncalves, S.; Castillo, J.; Fernández, A.; Hung, J. Absorbance and Fluorescence Spectroscopy on the Aggregation Behavior of Asphaltene-Toluene Solutions. *Fuel* **2004**, 83 (13), 1823–1828.

(51) Putman, J. C.; Gutiérrez Sama, S.; Barrère-Mangote, C.; Rodgers, R. P.; Lobinski, R.; Marshall, A. G.; Bouyssière, B.; Giusti, P. Analysis of Petroleum Products by Gel Permeation Chromatography Coupled Online with Inductively Coupled Plasma Mass Spectrometry and Offline with Fourier Transform Ion Cyclotron Resonance Mass Spectrometry. *Energy and Fuels* **2018**, 32 (12), 12198–12204.

(52) Acevedo, N.; Moulian, R.; Chacón-Patiño, M. L.; Mejia, A.; Radji, S.; Daridon, J. L.; Barrère-Mangote, C.; Giusti, P.; Rodgers, R. P.; Piscitelli, V.; Castillo, J.; Carrier, H.; Bouyssiere, B. Understanding Asphaltene Fraction Behavior through Combined Quartz Crystal Resonator Sensor, FT-ICR MS, GPC ICP HR-MS, and AFM Characterization. Part I: Extrography Fractionations. *Energy and Fuels* **2020**, 34 (11), 13903–13915.

(53) Aref Abbasi, M. Asphaltene induced changes in rheological properties: A review. *Fuel* **2022**, 316, 123372.

(54) Khalesi, M.; Yarranton, H.W.; Natale, G. Interfacial micro and macro rheology of fractionated asphaltenes. *Colloids and surfaces A: physicochemical and technical aspects* **2022**. 651, 12965.

(55) Yajian, W.; Wentao, W.; Linbing, W. Understanding the relationships between rheology and chemistry of asphalt binders: A review. *Construction and Building Materials* **2022**, 329, 127161.

(56) Danuta, M. S.; Harvey, W. Y. Rheology of Asphaltene−Toluene/Water Interfaces. *Langmuir* **2005**, 21,11651-11658.

(57) Villegas, O.; Vallverdu, G. S.; Bouyssiere, B.; Acevedo, Ś.; Castillo, J.; Baraille, I. Cancellation of Dipole Moment of Models of Asphaltene Aggregates as a Mean for Their Dispersion in Toluene and THF Calculated Using Molecular Dynamics. *Fuel* **2022**, 334, 126472.

(58) Villegas, O.; Salvato Vallverdu, G.; Bouyssiere, B.; Acevedo, S.; Castillo, J.; Baraille, I. Aggregation of Asphaltene Subfractions A1 and A2 in Different Solvents from the Perspective of Molecular Dynamics Simulations. *Energy and Fuels* **2023**, 37 (4), 2681–2691.

6. SUPPORTING INFORMATION

Representative AFM images height (1,5 μm × 1,5 μm), and cross-sections (white lines in the topography panels) and the height distributions of aggregates; AFM images of different aggregation types and force curves of the AFM force curves performed to determine the viscoelasticity for Cerro Negro, Hamaca and Furrial sample.